Electrochimica Acta xxx (2009) xxx–xxx

Contents lists available at ScienceDirect

Electrochimica Acta

journal homepage: www.elsevier.com/locate/electacta

Copper deposition onto silicon by galvanic displacement: Effect of Cu complex formation in NH_4F solutions

Calvin P. daRosa, Enrique Iglesia, Roya Maboudian*

Department of Chemical Engineering, University of California, 201 Gilman Hall, Berkeley, CA 94720, United States

ARTICLE INFO

Article history:
Received 26 August 2008
Received in revised form
21 November 2008
Accepted 18 December 2008
Available online xxx

Keywords:
Galvanic displacement
Electroless deposition
Open-circuit potential (OCP)
Rotating-disk electrode
Metallization

ABSTRACT

Copper was deposited onto rotating Si substrates by galvanic displacement in 6.0 M NH_4F to determine the effects of Cu complex formation on deposition rates. Deposition rates decreased with increasing rotation speed, indicating that Cu(I) intermediates, stabilized by NH_3, diffuse away from the Cu surface before they reduce to Cu(0). UV–visible spectra of contacting solutions and direct measurements of mass changes resulting from Cu deposition and Si removal confirmed this proposal. These findings contrast those reported previously for deposition from HF solutions, in which Cu(I) species are unstable and reduce rapidly to Cu(0). These data and mixed-potential theory were used to develop a reaction-transport model that accurately describes the effects of mass transfer and electrochemical reaction rates on Cu deposition dynamics and open-circuit potential (OCP) values. The effects of ascorbic acid and tartrate additives on film properties and formation rates were also examined. Cu reduction kinetics decreased significantly when ascorbic acid (0.01 M) was present. Adhesion of Cu films was improved when ascorbic acid was used, but internal stresses caused films to distort when their thicknesses exceeded 100 nm. Adding potassium sodium tartrate to solutions containing ascorbic acid decreased film stresses and led to robust films with excellent adhesion.

1. Introduction

Galvanic displacement has been used to selectively deposit Cu and other metals onto Si in many devices, such as integrated circuits, microelectromechanical systems, and microchannel chemical reactors [1–5]. HF is commonly used to dissolve oxidized Si in these systems, but NH_4F is an attractive alternative, because the near-neutral pH prevalent in NH_4F solutions allows deposition of less noble metals, such as Ni. In addition, NH_4F solutions are compatible with additives, such as ascorbic acid, that have been found to improve film adhesion to substrates [6–8]. The effects of NH_4F on mass transfer and kinetic processes involved in Cu galvanic displacement are examined here to determine appropriate conditions for the deposition of Cu films from NH_4F solutions.

NH_3 formed in NH_4F dissociation reacts with both Cu(II) and Cu(I) cations to form complexes, a process that stabilizes these species relative to the respective hydrated cations [9,10]. This effect is especially pronounced for Cu(I) species, which are much less stable than Cu(II) as hydrated cations in aqueous media, but more stable than Cu(II) as ammine complexes in NH_4F solutions [10]. As a result, the deposition model developed for galvanic displacement in HF solutions (Fig. 1a) must be modified, because Cu(II) reduction to Cu(0) cannot be treated as an irreversible single-step. Fig. 1b depicts the corresponding model for galvanic displacement in NH_4F solutions. In this case, the stable Cu(I) intermediates formed during Cu(II) reduction can diffuse away from the Cu surface before reduction to form Cu(0) films. The removal of Cu(I) before deposition has been proposed to account for the low Cu metal yields in electrodeposition from NH_3 solutions [11]. Here, we use the processes depicted in Fig. 1b to determine the influence of mass transfer and reaction kinetics on the rate of Cu deposition onto rotating Si substrates in 6 M NH_4F solutions.

Previous studies have shown that additives, such as ascorbic acid, potassium sodium tartrate, and methanol co-solvents improve the properties of Cu films on Si, via processes that remain incompletely understood [3,7]. Additives can affect deposition via formation of complexes with metal cations, adsorption onto electrode surfaces, or modification of the interfacial tension of the electrode [12]. Here, interactions between additives and Cu cations are determined by combining measurements of UV–visible spectra of deposition solutions, open-circuit potential (OCP) values, and Cu deposition rates. The effects of additives on reaction and mass transfer rates are used to elucidate their mechanism of action and to provide insights into deposition conditions that improve film properties. Ultimately, the structure of Cu films guides their function, and atomic-force and optical microscopies are used to determine the influence of these additives on film structure and on its consequences for adhesion and mechanical integrity.

* Corresponding author. Tel.: +1 510 6437957; fax: +1 510 6424778.
E-mail address: maboudia@berkeley.edu (R. Maboudian).

0013-4686/$ – see front matter © 2008 Elsevier Ltd. All rights reserved.
doi:10.1016/j.electacta.2008.12.037

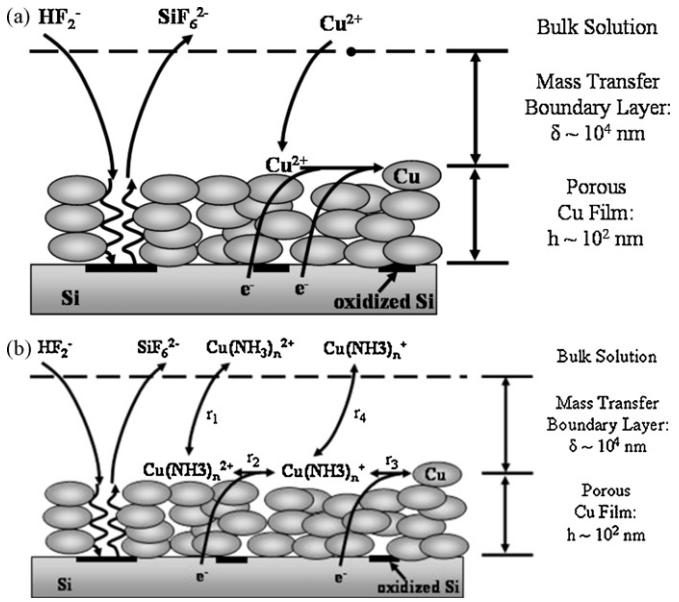

Fig. 1. Reaction-transport model for Cu deposition onto Si by galvanic displacement. (a) Previously developed model for deposition in HF solutions, where Cu^{2+} is irreversibly reduced to Cu^0 and (b) deposition model for NH_4F solutions, in which Cu^+ forms stable complexes with NH_3 which can either reduce further to Cu^0 or diffuse away from the Cu surface and into the bulk solution.

2. Experimental methods

Experimental methods were similar to those reported previously for deposition of Cu onto Si from HF solutions [13,14]. $CuSO_4{\cdot}5H_2O$ (99.3%, Fisher) was used as the Cu source (0.0010–0.020 M); NH_4F (Sigma–Aldrich, 40% w/w) was used as a 6.0-M aqueous solution to dissolve oxidized Si. The role of additives was studied by adding compounds previously reported to improve the adhesion of Cu films onto Si(7). These moieties were methanol (CH_3OH, Fisher, 99.8%), potassium sodium tartrate ($KNaC_4H_4O_6{\cdot}4H_2O$, Alfa Aesar, 99%), and ascorbic acid ($C_8H_8O_6$, Alfa Aesar, 99%). Deposition was carried out on ~1 cm^2 Si(1 0 0) substrates (ρ = 10–20 Ω cm; Wafernet, Inc.) attached to the end of a rotating shaft (Model A5R2, Pine Instruments). Rotation speeds were varied between 0 and 260 rad s^{-1} (2500 rpm). Open-circuit potential (OCP) values were measured using a high-impedance voltmeter (Keithley 2400 SourceMeter), and Hg/Hg_2SO_4 (REF621, Radiometer Analytical; 0.64 V vs. NHE) was used as the reference electrode.

The structures of Cu surfaces and of the underlying Si were assessed by atomic-force microscopy (Digital Instruments Multi-Mode III) in tapping mode. For these, experiments, Si surfaces were exposed by dissolving the Cu films in 0.5 M HNO_3 (69.5%, Fisher). AFM was also used to measure the thickness of Cu films, using the following method. Cu films were scratched with Teflon tweezers to expose the Si underneath, and the height difference at the Cu–Si interface was determined by AFM. Film thicknesses were used to calculate Cu deposition rates, assuming Cu void fractions of 0.15, as found previously [13]. Optical images were obtained with a Mitutoyo Finescope at 20× magnification; images were recorded using a CCD camera (Sony SSC-C370).

Solution compositions were determined from UV–visible spectra of solutions at wavelengths of 450–850 nm (Cary 400 Spectrometer). Cu(II) concentrations were found by removing 1-cm^3 aliquots from solution during deposition and measuring the absorbance at 690 nm. Polystyrene semi-micro cuvettes (International Crystal Laboratories) with 1 cm path length were used. Concentrations of Si(IV) in solution were then determined by adding $(NH_4)_2MoO_7$ (10% w/v in H_2O, Alfa Aesar) to each aliquot to form colored molybdosilicic acid [15]. Si(IV) concentrations were calibrated using samples with known concentrations of $H_2SiF_6^{2-}$ (Alfa Aesar, 35% w/w aqueous solution).

The amounts of Cu deposited and Si dissolved were also determined by measuring mass changes in the Si wafers used in UV–visible experiments. First, the mass of a Si sample was measured (±0.1 mg) using an analytical balance (Model A-250, Denver Instrument Company). After deposition, the sample was rinsed, dried, and weighed again. The Cu film was then dissolved by contact with 0.5 M HNO_3 for 60 s and the Cu-free Si sample was weighed again. The amount of Si dissolved during galvanic displacement was determined from the difference between this final mass and its initial value. The mass of Cu deposited was measured from the difference in mass before and after dissolving the Cu film. The amounts of Cu deposited and of Si dissolved determined from UV–visible spectra and mass changes agreed to within 20%.

3. Results and discussion

3.1. Copper deposition mechanism in 6.0 M NH_4F

Cu was deposited onto rotating Si substrates in 6.0 M NH_4F to determine the effect of mass transfer on Cu deposition rates. Deposition rates decreased with increasing rotation speeds in 0.010 M $CuSO_4$ solutions (Fig. 2). These results are in marked contrast with the higher reaction rates typically observed because of thinning of boundary layers as shear rates increase with increasing rotation speed [13]. The reaction transport-model proposed previously to describe galvanic displacement rates in HF solutions [13] (Fig. 1a) cannot account for these trends in deposition rates with increasing rotation speed for NH_4F solutions. The model is extended here to NH_4F solutions by accounting for the diffusion of Cu(I) cations away from the electrode surface and into the bulk solution (Fig. 1b) before they reduce to form Cu(0) films. Cu(I) complexes with NH_3 are more stable than either hydrated Cu(I) or Cu(II)–NH_3 complexes (Table 1). Previously reported calculations of equilibrium in Cu–NH_3–H_2O systems showed that a Cu(I) species, $Cu(NH_3)_2^+$, is the predominant ionic species in equilibrium with Cu(0) dur-

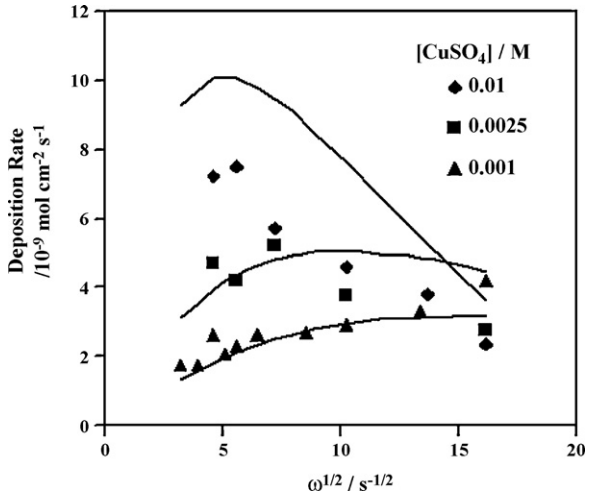

Fig. 2. Effect of mass transfer rates on Cu deposition rates. $[NH_4F]$ = 6.0 M; $[CuSO_4]$ = 0.010 M (♦), 0.0025 M (■), and 0.0010 M (▲); deposition time = 180 s. Deposition rates decrease with increasing mass transfer rates in high $CuSO_4$ concentrations, but increase in more dilute $CuSO_4$. Solid lines indicate deposition rates predicted from deposition model depicted in Fig. 1b and the associated Eqs. (11)–(14). This model captures the trends of decreasing deposition rates at high rotation speeds in 0.01 M $CuSO_4$ and increasing deposition rates with increasing rotation speeds in 0.001 M $CuSO_4$.

Please cite this article in press as: C.P. daRosa, et al., Copper deposition onto silicon by galvanic displacement: Effect of Cu complex formation in NH_4F solutions, Electrochim. Acta (2009), doi:10.1016/j.electacta.2008.12.037

Table 1
Standard Gibbs free energies of formation (ΔG_f°), stability constants (K), and reduction potentials (E°) of Cu ions in NH_3 solutions.

Cationic species	ΔG_f° (kJ mol^{-1})	$K = \frac{[Cu(NH_3)_m^{\nu+}]}{[Cu^{\nu+}][NH_3]^m}$	E° (V) vs. NHE
Cu^{2+}	65.0	–	0.337
$Cu(NH_3)^{2+}$	13.9	2.0×10^4	0.21
$Cu(NH_3)_2^{2+}$	−33.5	9.5×10^7	0.10
$Cu(NH_3)_3^{2+}$	−77.3	1.05×10^{11}	0.01
$Cu(NH_3)_4^{2+}$	−116.7	2.09×10^{13}	−0.06
Cu^+	50.3	–	0.521
$Cu(NH_3)^+$	−10.1	8.5×10^5	0.17
$Cu(NH_3)_2^+$	−64.7	7.2×10^{10}	−0.12

Data are taken from [10].

ing deposition in 6 M NH_4F [16,17]. The low reactivity of Cu(I)–NH_3 species allows their diffusion into bulk solutions before reduction and deposition as Cu(0). Similar effects were previously proposed to explain the decrease in deposition rates with increasing rotation speed for $Zn(OH)_2$ film growth on Zn [18]. In contrast to the results for 0.010 M $CuSO_4$, deposition rates increased with increasing rotation speeds in more dilute 0.0010 M $CuSO_4$. This suggests that Cu(I) species reduce before they can diffuse into the bulk solution at these lower $CuSO_4$ concentrations.

Steady-state model equations for the processes depicted in Fig. 1b were used to describe the effects of mass transfer and reaction kinetics on Cu deposition rates and OCP values. In the discussion that follows, ionic species are denoted as Cu(II) and Cu(I), irrespective of the solvating species (H_2O or NH_3) or number of NH_3 ligands. The effects of rotation speed on boundary layer mass transfer coefficients (k_m) are given by [19]

$$k_m = 0.62\nu^{-1/6}D^{2/3}\omega^{1/2} = k'\omega^{1/2} \tag{1}$$

where ν is the solution kinematic viscosity (in cm^2 s^{-1}), D is the diffusivity of a given species (in cm^2 s^{-1}), and ω is the angular velocity of rotation (in rad s^{-1}). Thus, Cu(II) diffusion rates from solutions to Cu or Si solid surfaces are given by

$$r_1 = k'_{Cu(II)}\omega^{1/2}\left\{[Cu(II)]_{bulk} - [Cu(II)]_{surface}\right\} \tag{2}$$

where $[Cu(II)]_{bulk}$ and $[Cu(II)]_{surface}$ denote the Cu(II) activities in the bulk solution and at the solid surface, respectively. Cu(II) is then reduced to Cu(I) by electrons formed by oxidation of Si [20]:

$$Cu(II)_{(surface)} + e^- \leftrightarrow Cu(I)_{(surface)} \tag{3}$$

$$r_2 = k_2^0\left\{[Cu(II)]_{surface}\ \exp\left[-\frac{\alpha F}{RT}\left(E - E_2^0\right)\right] - [Cu(I)]_{surface}\ \exp\left[\frac{(1-\alpha)F}{RT}\left(E - E_2^0\right)\right]\right\} \tag{4}$$

In Eq. (4), k_2^0 is the standard rate constant (the rate constant for the forward and reverse reactions at the standard potential and unit activities of Cu(II) and Cu(I)), E_2^0 is the standard potential of r_2 (0.16 V), α is the transfer coefficient (reflecting the symmetry of the electron transfer energy barrier), F is Faraday's constant (96,485 C (mol e$^-$)$^{-1}$), R is the gas constant (8.314 J mol^{-1} K^{-1}), T is the temperature in K, and E is the electrode open-circuit potential (OCP). The parameter Ψ denotes the extent to which Cu(I) formation rates are limited by boundary-layer mass transfer:

$$\Psi = \frac{k'_{Cu(II)}\omega^{1/2}}{k_2^0\exp\left[-(\alpha F/RT)(E - E_2^0)\right]} \approx \frac{r_1}{r_2} \tag{5}$$

Cu(II) mass transfer limits rates as $\Psi \to 0$, while Cu(II) reduction limits rates as $\Psi \to \infty$.

The Cu(I) species formed by reduction of Cu(II) can be reduced further to Cu(0), which then deposits onto the growing film [20]:

$$Cu(I)_{(surface)} + e^- \leftrightarrow Cu^{(0)} \tag{6}$$

$$r_3 = k_3^0\left\{[Cu(I)]_{surface}\exp\left[-\frac{\alpha F}{RT}\left(E - E_3^0\right)\right] - \exp\left[\frac{(1-\alpha)F}{RT}\left(E - E_3^0\right)\right]\right\} \tag{7}$$

The stable nature of Cu(I)–NH_3 species decreases their reduction rates and allows them to diffuse into the bulk solution before reaction at a rate given by

$$r_4 = k'_{Cu^+}\left\{[Cu(I)]_{surface} - [Cu(I)]_{bulk}\right\} \tag{8}$$

If bulk Cu(I) concentrations are much lower than those at the solid surface, the ratio of the Cu(I) diffusion rate (r_4 in Fig. 1b, Eq. (8)) to the rate for Cu(I) reduction to Cu(0) (r_3 in Fig. 1b, Eq. (7)) is given by the parameter Φ:

$$\Phi = \frac{k'_{Cu(I)}\omega^{1/2}}{k_3^0\ \exp\left[-(\alpha F/RT)(E - E_3^0)\right]} \approx \frac{r_4}{r_3} \tag{9}$$

This parameter reflects the selectivity of Cu(I) reduction to Cu(0): Cu^+ is selectively reduced to Cu(0) as $\Phi \to 0$, while Cu^+ cations diffuse into the bulk solution essentially unreacted for $\Phi \to \infty$.

Mixed-potential theory was used to estimate deposition rates and OCP values by equating the oxidation and reduction currents, a requirement of steady-state [21]. Current densities (i, in A cm^{-2}) are related to reaction rates (r, in mol cm^{-2} s^{-1}) by Faraday's law:

$$i = nFr \tag{10}$$

where n is the number of electrons transferred in the electrochemical half-reaction. It was shown previously that during galvanic displacement, Si is oxidized in a two-electron process, with subsequent oxidation to the stable SiF_6^{2-} product occurring in solution via H^+ reduction to H_2 [13]. The rate for Si oxidation followed by dissolution at the electrode surface is given by [22,23]

$$\frac{i_{Si}}{F} = 2r_{Si} = \frac{2k_{HF_2}[HF_2^-]k_{Si}^0\ \exp\left[(F/RT)(E - E_{Si}^0)\right]}{k_{HF_2}[HF_2^-] + k_{Si}^0\ \exp\left[(F/RT)(E - E_{Si}^0)\right]} \tag{11}$$

where $[HF_2^-]$ values were calculated from solution thermodynamics and found to be 0.015 M [24,25].

Cu reduction rates were determined from Eqs. (2) to (9) by assuming pseudo steady-state for Cu(II) and Cu(I) thermodynamic activities at Cu surfaces. At the potentials prevalent during deposition, the rate of the reverse (oxidation) reaction in Eq. (4) is much lower than the rate of reduction, and thus Cu(II) reduction to Cu(I) (Eqs. (3) and (4)) was assumed to be irreversible. The rates of Cu(II) diffusion and reduction (Eqs. (2) and (4)) can then be combined to find the current density for reduction of Cu(II) to Cu(I):

$$\frac{i_{Cu(II)\to Cu(I)}}{F} = \frac{k'_{Cu(II)}\omega^{1/2}k_2^0\ \exp\left[-(\alpha F/RT)(E - E_2^0)\right][Cu(II)]_b}{k'_{Cu(II)}\omega^{1/2} + k_2^0\ \exp\left[-(\alpha F/RT)(E - E_2^0)\right]} = \frac{k'_{Cu(II)}\omega^{1/2}[Cu(II)]_b}{1 + \Psi} \tag{12}$$

Similarly, the net current density for Cu(I) reduction to Cu(0) (Eqs. (6) and (7)) is

$$\frac{i_{Cu(I)\to Cu(0)}}{F} = \frac{k'_{Cu(II)}\omega^{1/2}[Cu(II)]_b}{(1+\Psi)(1+\Phi)} - \left(\frac{\Phi}{1+\Phi}\right)k_3^0\ \exp\left[\frac{(1-\alpha)F}{RT}(E - E_3^0)\right] \tag{13}$$

Please cite this article in press as: C.P. daRosa, et al., Copper deposition onto silicon by galvanic displacement: Effect of Cu complex formation in NH_4F solutions, Electrochim. Acta (2009), doi:10.1016/j.electacta.2008.12.037

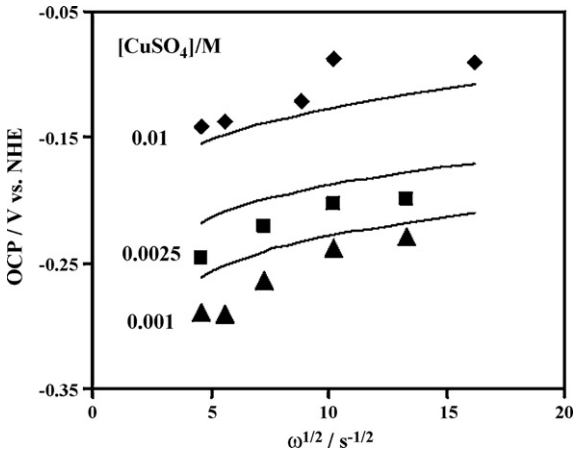

Fig. 3. Comparison of OCP values measured during deposition and values calculated from Eqs. (11)–(14). [NH_4F] = 6.0 M, [$CuSO_4$] = 0.010 M (♦), 0.0025 M (■), and 0.0010 M (▲).

The first term on the right-hand side of Eq. (13) represents the rate of Cu(I) reduction to Cu(0), and the second term represents the reverse reaction. The step-wise reduction currents in Eqs. (12) and (13) can then be added to yield the total Cu reduction current:

$$\frac{i_{Cu,total}}{F} = \frac{k'_{Cu^{2+}}\omega^{1/2}[\mathrm{Cu(II)}]_b}{1+\Psi}\left(1+\frac{1}{1+\Phi}\right) - \left(\frac{\Phi}{1+\Phi}\right)k_3^0 \exp\left[\frac{(1-\alpha)F}{RT}(E-E_3^0)\right] \quad (14)$$

The mixed potential, E, was calculated by setting the total Cu reduction current (Eq. (14)) equal to the Si oxidation current (Eq. (11)).

Because electrons cannot be generated or destroyed, the rate at which electrons are liberated in the Si oxidation reaction (Eq. (11)) must equal the rate at which they are consumed in the Cu reduction reactions (Eq. (14)). OCP values were predicted by solving iteratively for the potential E that satisfied the condition that the currents given by Eqs. (11) and (14) (i_{Si} and i_{Cu} respectively) are equal to each other for each $CuSO_4$ concentration and rotation speed considered. This potential was then substituted into Eq. (13) to find the predicted rate of Cu deposition. These results agree qualitatively with measured rates as functions of $CuSO_4$ concentration and rotation speed (Fig. 2). The model correctly predicts a decrease in deposition rate with increasing rotation speed in 0.010 M $CuSO_4$ solutions; measured rates, however, are slightly lower than predictions. This model also accurately predicts that deposition rates increase with increasing rotation speed at lower $CuSO_4$ concentrations (0.0010 M).

OCP values predicted by the deposition model also agree with measurements, namely OCP values increase with increasing rotation speed or $CuSO_4$ concentration (Fig. 3). Higher OCP values reflect a higher driving force for reduction [26], suggesting that the driving force for reduction increases with increasing rotation speed, in spite of lower measured deposition rates from 0.01 M $CuSO_4$ solutions. This is consistent with the expressions for Cu reduction rates given in Eqs. (13) and (14). The sum of the reduction rates of Cu(II) to Cu(I) and Cu(I) to Cu(0) (Eq. (14)) increases monotonically as rotation speed increases, but the rate of Cu(I) reduction and of concomitant Cu(0) deposition (Eq. (13)) decreases at high rotation speeds. The rate of Si oxidation and dissolution (Eq. (11)) must equal the total rate of Cu reduction (Eq. (14)) at steady state. Thus, the amount of Si dissolved must also increase with increasing rotation speed, a hypothesis that is confirmed below by measuring the mass change of Si substrates following deposition.

Cu deposition rates in 0.01 M $CuSO_4$ solutions decrease with increasing rotation speed because Cu(I) species diffuse away from surfaces before they react. Cu(0) deposition rates as given by Eq. (13) do not change monotonically with rotation speed because both Φ and Ψ are proportional to $\omega^{1/2}$. A schematic depiction of the effects of $\omega^{1/2}$ on Cu deposition rates is shown in Fig. 4. At low rotation speeds, mass transfer rates are low, and both Φ and $\Psi \ll 1$. Thus, Cu(II) reduction is limited by the rate of mass transfer to the electrode, and Cu(I) intermediates are reduced to Cu(0) before they can diffuse back to the bulk solution. At these low rotation speeds, Cu deposition rates are proportional to $\omega^{1/2}$. In contrast, at high rotation speeds, mass transfer rates are high and both Φ and $\Psi \gg 1$. As a result, the first term in Eq. (13) is proportional to $\omega^{-1/2}$, and deposition rates decrease with increasing rotation speed. In this case, Cu(II) reduction to Cu(I) is limited by reaction kinetics, not transport of Cu(II) to the electrode surface, so increasing ω does not increase the rate of Cu(I) generation. In contrast, the rate of Cu(I) diffusion to the bulk solution (r_4) is proportional to $\omega^{1/2}$, which decreases the rate of Cu(I) reduction to Cu(0) (r_3). This trend can be seen in Fig. 4, where r_3 decreases at high rotation speeds as r_4 increases.

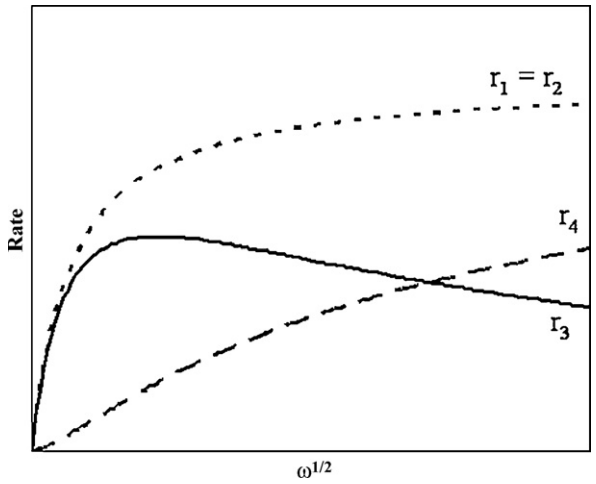

Fig. 4. Schematic depiction of the effect of rotation speed on the rate of processes depicted in Fig. 1b. r_1 is the rate of Cu(II) diffusion to the electrode surface. r_2 is the rate of Cu(II) reduction to Cu(I). r_1 and r_2 are equal at steady state. r_3 is the rate of Cu(I) reduction to Cu(0), and r_4 is the rate of Cu(I) diffusion from the electrode surface to the bulk solution. At steady state, Cu(I) is generated at the electrode surface at the same rate as it is removed by either reaction or diffusion: $r_2 = r_3 + r_4$.

The amounts of Cu deposited and of Si dissolved (determined by mass changes following deposition) were used to confirm that Si dissolution rates increase monotonically with increasing ω, as predicted above. The amount of Cu deposited decreased with increasing ω in 6.0 M NH_4F and 0.010 M $CuSO_4$ (Fig. 5), as also measured by AFM. Deposition rates were proportional to $1/\omega^{1/2}$, indicating that rates were limited by Cu(I) diffusion from film surfaces, as predicted by Eq. (13) for large Φ and Ψ values. The amount of Si dissolved, however, increased monotonically with increasing ω (Fig. 5), indicating a higher rate of reduction and oxidation. Since Si oxidation rates must balance the total rate of Cu reduction, the rate of Cu(II) reduction must also increase with increasing rotation speeds. Since the amount of Cu(0) deposited decreases with increasing rotation speeds, this demonstrates that Cu(II) species are reduced but not deposited as Cu(0) with increasing frequency as ω increases. This is consistent with the proposed deposition model, which indicates partially reduced Cu(I) species diffuse away from the electrode before further reduction can occur at high rotation speeds.

UV–visible spectra were also used to confirm the conclusion that Cu(II) is reduced more selectively to Cu(I) at high rotation speeds. Following deposition at $\omega = 100\ s^{-1}$ in a solution initially containing 0.01 M $CuSO_4$, the Cu(II) concentration was found to be 0.0070 M. This Cu(II) depletion would correspond to a Cu film thick-

Please cite this article in press as: C.P. daRosa, et al., Copper deposition onto silicon by galvanic displacement: Effect of Cu complex formation in NH_4F solutions, Electrochim. Acta (2009), doi:10.1016/j.electacta.2008.12.037

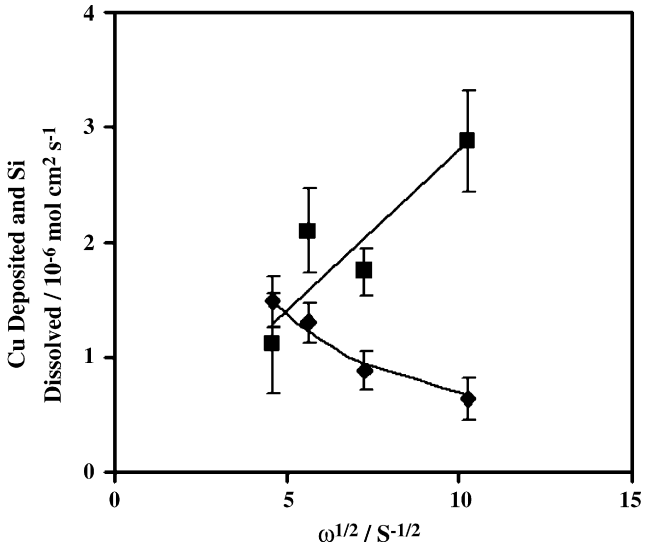

Fig. 5. Effect of rotation speed on amounts of Cu deposited (♦) and Si dissolved (■), determined from mass measurements. The solid lines are proportional to $\omega^{1/2}$ for Si and $\omega^{-1/2}$ for Cu, indicating the limiting cases for reaction limited by diffusion of reactants to the electrode and reaction limited by diffusion of an intermediate away from the electrode, respectively. [NH_4F] = 6.0 M, [$CuSO_4$] = 0.010 M, deposition time = 300 s.

ness of 1.3 μm (areal Cu density of 1.4×10^{-5} mol Cu cm^{-2}) if it were all incorporated into the film. Direct measurement by AFM, however, indicated a film thickness of only 250 nm. Thus, we conclude that Cu(II) forms species (e.g., Cu(I)) undetectable by UV–visible spectroscopy, but not Cu(0) solids. Aliquots of deposition solutions were exposed to ambient air for 4 h to oxidize any Cu(I) species present to Cu(II). The Cu(II) concentration measured after this interval was 0.0093 M. This degree of Cu(II) depletion corresponds to a film thickness of 275 nm (3.1×10^{-6} mol Cu cm^{-2}), in good agreement with the thickness measured by AFM. These data indicate that a significant fraction of Cu(II) was reduced only to Cu(I) without subsequent reduction to Cu(0). Further evidence that Cu(II) was partially reduced to Cu(I) without subsequent Cu deposition is seen in the SiF_6^{2-} concentration determined from UV–visible spectra. These results indicate that the areal density of Si removed from the electrode surface was 2.0×10^{-5} mol Si cm^{-2}. This is nearly an order of magnitude greater than the amount of Cu deposited and indicates that most of the Si that was oxidized and dissolved during the galvanic displacement process did not result in Cu deposition. These results are consistent with the findings from direct measurements of mass changes discussed above.

3.2. Effect of additives on Cu deposition behavior

The effects of solution additives on Cu deposition rates and OCP values are shown in Figs. 6 and 7, respectively. Deposition rates decreased with increasing rotation speed when CH_3OH was present, but these trends were much weaker than without CH_3OH. CH_3OH also decreased OCP values (Fig. 7), consistent with a higher reduction rate. This effect is strongest for reduction of Cu(I), because this step is closer to equilibrium than Cu(II) reduction. The absorbance of the deposition solution in the UV–visible range is higher and features move to lower wavelengths when CH_3OH is present, suggesting that Cu(II)–NH_3 complexes are more stable, as reported previously [27]. As a result, a lower potential is needed to reduce Cu^{2+} species, and the relative rate of Cu(I) reduction is then increased due to the lower potential. Therefore, less Cu(I) is able to diffuse away from near-surface regions, and Cu deposition rates do not decrease as sharply with increasing rotation speeds.

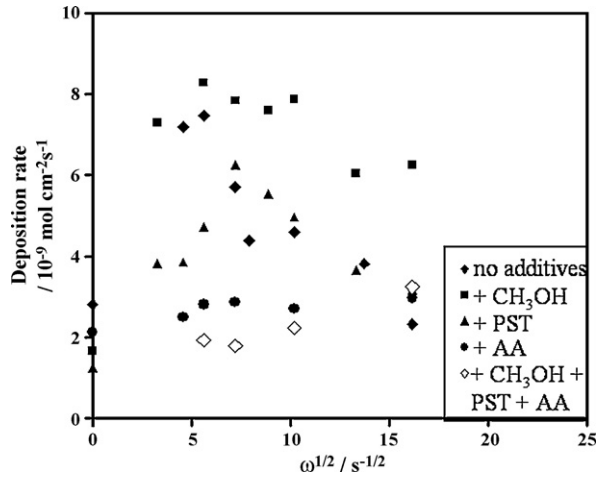

Fig. 6. Effect of rotation speed on deposition rates in solutions containing additives. Each solution contains 6.0 M NH_4F, 0.010 M $CuSO_4$, and the following additives: no additives (♦); 7.4 M CH_3OH (■); 0.01 M potassium sodium tartrate (▲); 0.01 M ascorbic acid (●); 7.4 M CH_3OH, 0.01 M potassium sodium tartrate, and 0.01 M ascorbic acid (◊). Deposition time = 180 s.

The presence of potassium sodium tartrate led to lower deposition rates with increasing rotation speed in 0.01 M $CuSO_4$, as also found with additive-free solutions (Fig. 6), suggesting similar reaction mechanisms apply in the two cases. Deposition rates were similar with and without tartrate at high rotation speeds, but tartrate led to lower deposition rates than additive-free solutions at low rotation speeds. This is apparently not due to the formation of Cu complexes with tartrate, because thermodynamic calculations indicate very little Cu(II) is present in tartrate complexes in the presence of NH_3. Thus, it is more likely that tartrate adsorption on Cu surfaces inhibits the reaction, as proposed previously [28].

Deposition behavior changes significantly in the presence of ascorbic acid. Deposition solutions changed from blue to colorless when ascorbic acid was added, indicating that Cu(II) species were reduced to Cu(I) by ascorbic acid. Solution pH remained virtually unchanged at 7 after 0.01 M ascorbic acid was added because of the much higher concentration of NH_4F (6 M), which acts as a buffer and suppresses changes in pH. The prevalence of Cu(I) cations in the bulk solution led to a monotonic increase in Cu deposition rates

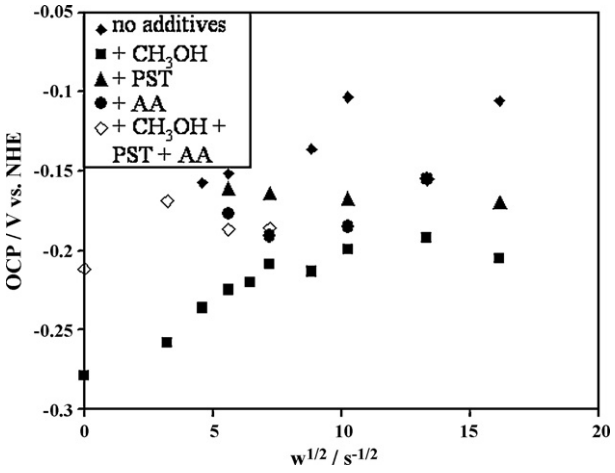

Fig. 7. Effect of rotation speed on OCP values in solutions containing additives. Each solution contains 6.0 M NH_4F, 0.010 M $CuSO_4$, and the following additives: no additives (♦); 7.4 M CH_3OH (■); 0.01 M potassium sodium tartrate (▲); 0.01 M ascorbic acid (●); 7.4 M CH_3OH, 0.01 M potassium sodium tartrate, and 0.01 M ascorbic acid (◊).

Please cite this article in press as: C.P. daRosa, et al., Copper deposition onto silicon by galvanic displacement: Effect of Cu complex formation in NH_4F solutions, Electrochim. Acta (2009), doi:10.1016/j.electacta.2008.12.037

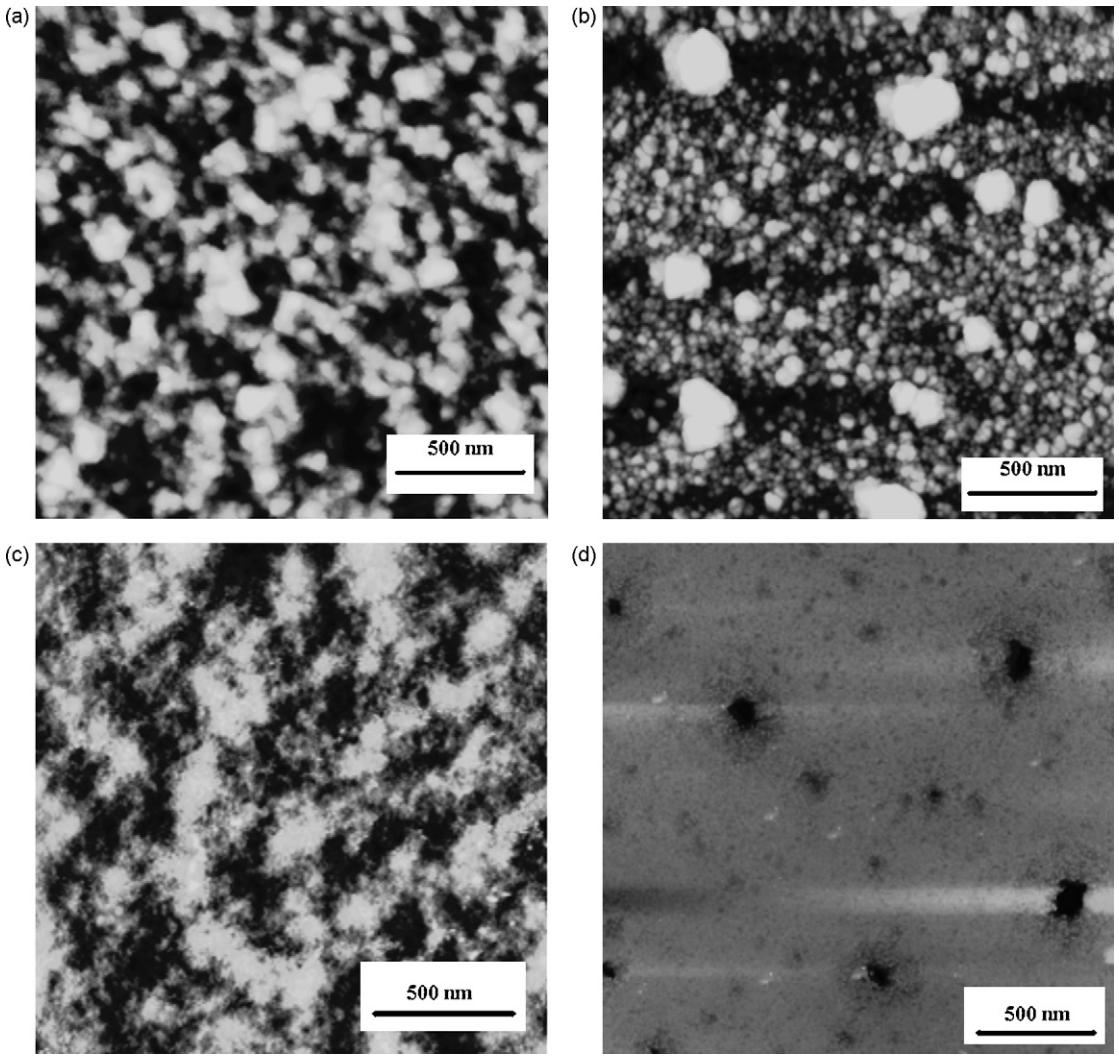

Fig. 8. AFM micrographs of surfaces of Cu films and Si substrates following deposition. [NH_4F] = 6 M, [$CuSO_4$] = 0.01 M, film thickness = 60 nm. (a) Cu surface following deposition with no additives. (b) Cu surface following deposition in solution containing 0.01 M ascorbic acid. (c) Underlying Si surface following deposition with no additives. (d) Underlying Si surface following deposition in solution containing 0.01 M ascorbic acid. Scan size is 2 μm × 2 μm, and the vertical scale is 50 nm in all images.

with increasing rotation speed (Fig. 6), because the rate of Cu(I) transport to the surface (r_4 in Fig. 1b) increased with rotation speed. Diffusion coefficients were estimated using the Koutecky–Levich Equation for mass transfer and chemical reaction in series [20]:

$$\frac{1}{r} = \frac{1}{k_{surface}C} + \frac{\nu^{1/6}}{0.62D^{2/3}C\omega^{1/2}} \quad (15)$$

where $k_{surface}$ is the surface reaction rate constant, and the other terms are as defined above. Based on this expression, plots of r^{-1} vs. $\omega^{-1/2}$ will be straight lines, with slopes proportional to $D^{-2/3}$ and y-intercepts proportional to $k_{surface}^{-1}$. Using the data for ascorbic acid solutions in Fig. 6, the Cu(I) diffusion coefficient calculated in this manner is $(4.6 \pm 2.0) \times 10^{-6}$ cm^2 s^{-1}, which agrees well with previous values (3.3×10^{-6} cm^2 s^{-1}) for Cu(I) complexes in NH_3 solutions [29]. Deposition rates were only ~10% of the maximum mass transfer rates estimated from these diffusion coefficients, which indicates deposition rates were not limited by mass transfer, but by Cu(I) reduction at the electrode surface. The surface reaction rate constant was estimated to be 3×10^{-4} cm s^{-1}. This values is ~10 times smaller than in the absence of ascorbic acid (3.8×10^{-3} cm s^{-1}), indicating that ascorbic acid strongly inhibits Cu(I) reduction to Cu(0).

3.3. Effect of additives on film properties

The effect of additives on Cu film properties was examined by AFM and optical microscopy. A typical AFM image of Cu film 60 nm in thickness deposited in 6.0 M NH_4F without additives is depicted in Fig. 8a. No surface features are apparent and height fluctuations vary randomly across the film surface. In contrast, Cu films deposited in 6.0 M NH_4F and 0.01 M ascorbic acid show large isolated features (~250 nm in diameter) that rise well above vicinal film surfaces (up to 40 nm) (Fig. 8b). Local galvanic displacement rates much higher at these asperities than mean values give rise to such inhomogeneities. AFM images of the underlying Si surface (exposed by Cu dissolution with HNO_3) are consistent with this hypothesis. Pits, occasionally >100 nm in depth, are evident on exposed Si surfaces after deposition from Cu solutions containing ascorbic acid (Fig. 8d). Deposition from additive-free solutions led instead to weaker fluctuations in the height of Si surfaces after deposition (Fig. 8c). Thus, Si dissolution rates appear to be locally enhanced by ascorbic acid, providing the electrons required to form the large features observed on the Cu surface. In addition, localized Si dissolution may contribute to the improved adhesion observed for Cu films deposited with ascorbic acid by maintaining intimate Cu–Si contact over a larger area of the Si substrate.

Please cite this article in press as: C.P. daRosa, et al., Copper deposition onto silicon by galvanic displacement: Effect of Cu complex formation in NH_4F solutions, Electrochim. Acta (2009), doi:10.1016/j.electacta.2008.12.037

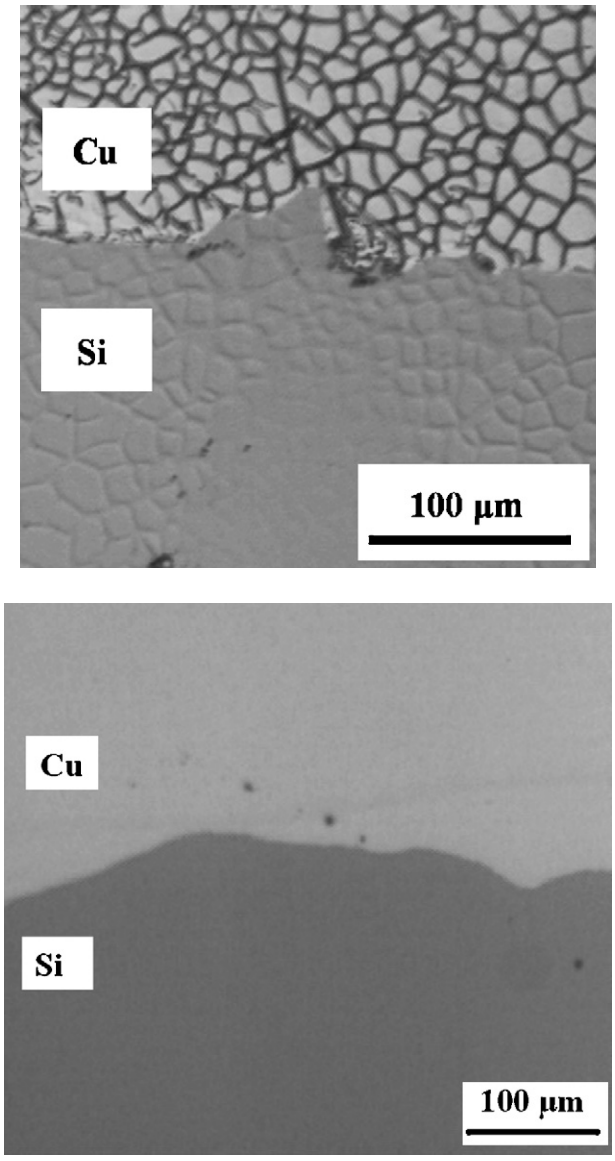

Fig. 9. Optical micrographs of ~100-nm thick Cu film deposited in 6 M NH_4F, 0.01 M $CuSO_4$ solutions. A portion of the Cu films were removed by scratching with tweezers to expose the Si in the lower half of the image. (a) 0.01 M ascorbic acid added; the dark lines on the Cu surface indicate locations where the Cu film restructured to decrease compressive stress. (b) 0.01 M ascorbic acid + 0.01 M potassium sodium tartrate added; no stress-induced restructuring is seen in these films.

Ascorbic acid improves the adhesion of thin Cu films, but leads to significant stresses in thick films (>100 nm). Optical micrographs show Cu surfaces with smooth 25-μm regions surrounded by dark grain boundaries (Fig. 9a). These boundaries are ~1 μm higher than the grains, suggestive of film restructuring to relieve compressive stresses developed during film growth [30]. A portion of the Cu film shown in Fig. 9a was removed by abrading with Teflon tweezers to reveal the underlying Si. The Si surface demonstrates features of approximately the same dimensions as Cu features, suggesting that Si dissolution is inhibited at such boundaries because of poor electronic contact between Cu and Si within these regions.

Potassium sodium tartrate (0.01 M) addition to solutions containing ascorbic acid (0.01 M) with or without CH_3OH led to reflective Cu films with excellent adhesion to Si substrates. These films do not exhibit the symptoms of compressive stress typical of films formed from solutions containing ascorbic acid but no tartrate (Fig. 9b), indicating that the primary role of tartrate is to relieve stresses in the Cu films, as proposed previously [28].

4. Conclusions

Copper films were deposited onto Si by galvanic displacement using 6.0 M NH_4F as the Si etchant and the effects of additives and Cu–NH_3 equilibrium on Cu deposition rates and film properties were examined. In the absence of additives, Cu deposition rates decreased with increasing rotation speed in 0.010 M $CuSO_4$, but increased with increasing rotation speed in 0.0010 M $CuSO_4$. A reaction-transport model was used to characterize the system. It was found that diffusion of the stable, partially reduced $Cu(NH_3)_2^+$ intermediate away from the Cu surface caused deposition rates to decrease as mass transfer rates increased in 0.01 M $CuSO_4$. Deposition rates and OCP values predicted from this mechanism agree qualitatively with the experimentally measured results. The proposed mechanism was also supported by mass measurements of Cu deposited and of Si dissolved. The mass of Cu deposited decreased with increasing rotation speed in 0.01 M $CuSO_4$ while the amount of Si dissolved increased, indicating additional Cu(II) reduction occurred without Cu^0 deposition.

The effects of the additives ascorbic acid and potassium sodium tartrate on Cu deposition behavior were also studied to determine their role in the deposition process and in improving the adhesion of Cu films to Si substrates. Ascorbic acid reduces Cu(II) species to Cu(I) in the bulk solution, as evidenced by the change in solution color from blue to clear. Deposition rates decreased significantly when ascorbic acid was present. This change was found to be caused by a decrease in reaction kinetics, and not diffusion rates. Cu films formed with ascorbic acid present demonstrated good adhesion to the Si substrate, but exhibited significant compressive stress. Adding potassium sodium tartrate to these solutions led to films with good adhesion and low internal stress.

Acknowledgements

We acknowledge Professor Elton Cairns of the University of California at Berkeley for access to the rotating disk electrode system used for the measurements reported here. This research was funded by the Committee on Research of the University of California at Berkeley, and the National Science Foundation. Mr. daRosa also thanks the National Science Foundation and the Chevron Corporation for fellowship support.

References

[1] J.G.A. Brito-Neto, S. Araki, M. Hayase, J. Electrochem. Soc. 153 (2006) C741.
[2] H. Cachet, M. Froment, E. Souteyrand, C. Dennig, J. Electrochem. Soc. 139 (1992) 2920.
[3] C. Carraro, R. Maboudian, L. Magagnin, Surf. Sci. Rep. 62 (2007) 499.
[4] C. Carraro, L. Magagnin, R. Maboudian, Electrochim. Acta 47 (2002) 2583.
[5] A.T. Carvalho, A.P. Nascimento, L.M. Silva, M.L.P. Silva, J.C. Madaleno, L. Pereira, Adv. Mater. Forum III (Pts 1 and 2) (2006) 1328.
[6] F.A. Harraz, T. Sakka, Y.H. Ogata, Phys. Stat. Sol. a: Appl. Res. 197 (2003) 51.
[7] L. Magagnin, R. Maboudian, C. Carraro, Electrochem, Solid State Lett. 4 (2001) C5.
[8] X. Zhang, F. Ren, M.S. Goorsky, K.N. Tu, Surf. Coat. Technol. 201 (2006) 2724.
[9] J. Bjerrum, C.J. Ballhausen, C.K. Jorgensen, Acta Chem. Scand. 8 (1954) 1275.
[10] J.A. Dean, Lange's Handbook of Chemistry, McGraw-Hill, New York, 1992.
[11] J. Sedzimir, M. Bujanska, Hydrometallurgy 3 (1978) 233.
[12] T.C. Franklin, Plat. Surf. Finish. 81 (1994) 62.
[13] C.P. daRosa, E. Iglesia, R. Maboudian, J. Electrochem. Soc. 155 (2008) D244.
[14] C.P. daRosa, R. Maboudian, E. Iglesia, J. Electrochem. Soc. 155 (2008) E70.
[15] Z. Marczenko, Separation and Spectrophotometric Determination of Elements, Halsted Press, New York, 1986.
[16] H.E. Johnson, J. Leja, J. Electrochem. Soc. 112 (1965) 638.
[17] J.M. Steigerwald, D.J. Duquette, S.P. Murarka, R.J. Gutmann, J. Electrochem. Soc. 142 (1995) 2379.

Please cite this article in press as: C.P. daRosa, et al., Copper deposition onto silicon by galvanic displacement: Effect of Cu complex formation in NH_4F solutions, Electrochim. Acta (2009), doi:10.1016/j.electacta.2008.12.037

[18] N. Diomidis, J.P. Celis, Surf. Coat. Technol. 195 (2005) 307.
[19] V.G. Levich, Physicochemical Hydrodynamics, Prentice-Hall, Englewood Cliffs, NJ, 1962.
[20] A.J. Bard, L.R. Faulkner, Electrochemical Methods: Fundamentals and Applications, Wiley, New York, 2001.
[21] C. Wagner, W.E. Traud, Z. Elektrochem. Angew. Phys. Chem. 44 (1938) 391.
[22] P.C. Searson, X.G. Zhang, J. Electrochem. Soc. 137 (1990) 2539.
[23] J. van den Meerakker, M.R.L. Mellier, J. Electrochem. Soc. 148 (2001) G166.
[24] R. Braddy, P.T. McTigue, B. Verity, J. Fluorine Chem. 66 (1994) 63.
[25] K.W. Kolasinski, J. Electrochem. Soc. 152 (2005) J99.
[26] G.P. Power, I.M. Ritchie, Electrochim. Acta 26 (1981) 1073.
[27] L.N. Trevani, J.C. Roberts, P.R. Tremaine, J. Solution Chem. 30 (2001) 585.
[28] I.A. Carlos, C.A.C. Souza, E. Pallone, R.H.P. Francisco, V. Cardoso, B.S. Lima-Neto, J. Appl. Electrochem. 30 (2000) 987.
[29] J. Penar, A. Persona, K. Sykut, Polish J. Chem. 70 (1996) 1329.
[30] M.D. Thouless, Annu. Rev. Mater. Sci. 25 (1995) 69.

Please cite this article in press as: C.P. daRosa, et al., Copper deposition onto silicon by galvanic displacement: Effect of Cu complex formation in NH_4F solutions, Electrochim. Acta (2009), doi:10.1016/j.electacta.2008.12.037